Polar Science 46 (2025) 101255

Contents lists available at ScienceDirect

Polar Science

journal homepage: www.elsevier.com/locate/polar

Influence of early sea ice melting on the autumn microplankton community of the Pacific Arctic Ocean

Kohei Sumiya [a], Dai Sumiyoshi [a,*], Kazutoshi Sato [b], Akihiko Murata [c], Shigeto Nishino [c], Kohei Matsuno [a,d]

[a] Faculty/Graduate School of Fisheries Science, Hokkaido University, 3-1-1 Minato-cho, Hakodate, Hokkaido, 041-8611, Japan
[b] International Polar and Earth Environmental Research Center, National Institute of Polar Research, 10-3 Midori-cho, Tachikawa, Tokyo, 190-8518, Japan
[c] Research Institute for Global Change, Japan Agency for Marine-Earth Science and Technology (JAMSTEC), 2-15 Natsushima-Cho, Yokosuka, Kanagawa, 237-0061, Japan
[d] Arctic Research Center, Hokkaido University, Kita-21 Nishi-11, Kita-ku, Sapporo, Hokkaido, 001-0021, Japan

ARTICLE INFO

Keywords:
Diatoms
Dinoflagellates
Ciliates
Leptocylindrus spp.
Cylindrotheca closterium

ABSTRACT

Sea ice in the Pacific Arctic Ocean has been rapidly decreasing over recent decades. However, knowledge of its effects on microplankton is limited. To elucidate the effect of sea ice reduction on the microplankton community of the Pacific Arctic Ocean, we examined the differences in the microplankton community and hydrography between 2019 and 2020. Based on the cluster analysis, the microplankton community was divided into six groups. In the southern Chukchi Sea, high cell densities were observed with high variability in group occurrence owing to the inflow of nutrient-rich Pacific water. In the northern Chukchi Sea, a 1-month inter-annual difference in sea ice melting timing induced changes in the microplankton community through hydrographical changes. Early sea ice melting stimulates the growth of phytoplankton species (*Proboscia alata*), which can utilize organic nitrogen compounds. In the marginal ice zone, a 10-day inter-annual difference in sea ice melting was observed, resulting in variations in hydrographic conditions; however, these changes did not affect the microplankton community. Our findings indicate that microplankton production and diversity respond differently to sea ice melting in varies by region in the Pacific Arctic Ocean.

1. Introduction

Sea ice in the Arctic Ocean has notably decreased over the past several decades, resulting in a considerably longer melting period (Stroeve et al., 2007; Comiso et al., 2008; Kwok and Rothrock, 2009; Zheng et al., 2021). The reduction in sea ice extent has increased the area and duration suitable for phytoplankton growth. Satellite observations indicate that the annual primary production in the entire Arctic Ocean has increased by 57 % from 1998 to 2018 (Lewis et al., 2020; Shiozaki et al., 2022). This is a remarkable trend in the shelf of the Pacific Arctic Ocean (Arrigo et al., 2008; Pabi et al., 2008; Arrigo and van Dijken, 2015).

The Pacific Arctic Ocean is categorized into shelf and basin areas based on bathymetric depth. The Chukchi Sea, a shallow (approximately 60 m) shelf area, connects the Pacific and Arctic Oceans and exhibits one of the highest primary productions in the Arctic Ocean owing to the inflow of nutrient-rich Pacific water (McRoy, 1993; Springer and McRoy, 1993). In contrast to this high primary production, the low feeding pressure exerted by zooplankton in the water column results in most phytoplankton descending to the seafloor, leading to the formation of localized high-density communities of benthos that feed on the settled phytoplankton (Grebmeier et al., 1988, 2006; Springer and McRoy, 1993). Furthermore, it is a highly productive area worldwide, with an abundance of higher trophic level organisms such as seabirds and marine mammals that feed on the benthos (Springer et al., 1996).

In the shelf area, ice algae production (mainly pennate diatoms) occurs in and under sea ice from April to June and rapidly proliferates with the melting of sea ice (Giesbrecht et al., 2019). Following the retreat of sea ice during summer, an increase in light penetrating through the ocean surface occurs. The influx of meltwater from sea ice

Abbreviations: SCM, sub-surface chlorophyll *a* maximum layer; CTD, conductivity–temperature–depth measurements; TSM, time since sea-ice melt; BCSW, Bering–Chukchi Summer Water; BCWW, Bering–Chukchi Winter Water; MW, Melt Water; MIZ, marginal ice zone; AW, Anadyr Water; ACW, Alaskan Coastal Water.

* Corresponding author.
E-mail address: sumiyoshi.dai.u5@elms.hokudai.ac.jp (D. Sumiyoshi).

https://doi.org/10.1016/j.polar.2025.101255
Received 3 October 2024; Received in revised form 3 July 2025; Accepted 8 July 2025
Available online 8 July 2025

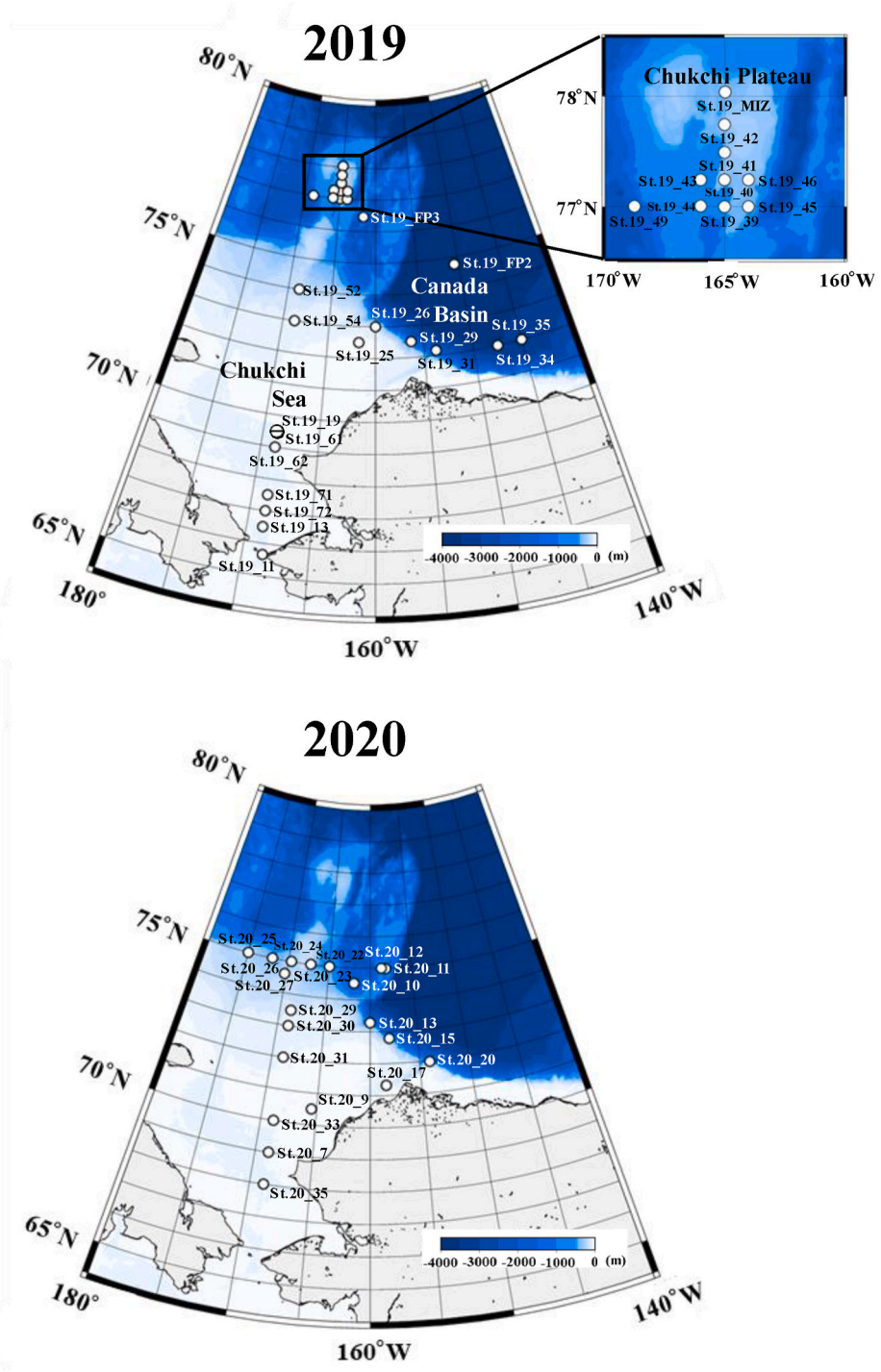

Fig. 1. Location of sampling stations in the Pacific sector of the Arctic Ocean during autumn 2019 and 2020.

stratifies the surface water, increases the residence time of phytoplankton within the surface layer, and creates favorable light conditions, that enable phytoplankton proliferation (mainly centric diatoms, such as *Chaetoceros* spp. and *Thalassiosira* spp.) (Horner and Schrader, 1982; Horner, 1984; Sakshaug, 1997; Hill and Cota, 2002; Arrigo et al., 2014). Increases in the frequency and area of autumn blooms (Ardyna et al., 2014) have also been reported in addition to conventional spring blooms. In recent autumn seasons, seafloor blooms composed mainly of *Thalassiosira* spp. and *Navicula* spp. have been observed in the shelf area due to increase light reaching the seafloor caused by sea ice reduction, and these blooms may be detected as SCM and could exhibit higher chlorophyll *a* (chl. *a*) concentration values than those at the surface (Shiozaki et al., 2022). Wind-driven autumn blooms have also been reported, in which strong winds mix the surface water and supply nutrients to the surface layer from the bottom layer, leading to the proliferation of micro phytoplankton, mainly *Cylindrotheca closterium* and *Leptocylindrus danicus* (Matsuno et al., 2015; Nishino et al., 2015; Yokoi et al., 2016).

In contrast, deep basin areas exhibit low productivity throughout the year (Arrigo et al., 2008) and decreased primary production owing to the inflow of nutrient-depleted water from the shelf area and strong stratification (Arrigo and van Dijken, 2015). The Canada Basin typically

has a well-developed halocline with low salinity, low nutrients, and relatively warm temperatures in the shallow layer, as well as high salinity, high nutrients, and low temperatures deeper than the halocline (Aagaard et al., 1981). Recently, the decrease in sea ice and increase in freshwater volume owing to river water inflows have contributed to a deepening of the nutricline in the basin and strengthened the stratification, which may negatively affect primary production (McLaughlin and Carmack, 2010).

Phytoplankton communities in the Pacific Arctic Ocean are dominated by diatoms (Sergeeva et al., 2010; Giesbrecht et al., 2019). Diatoms exhibit species-specific growth rates, carbon uptake rates, and photosynthetic efficiencies (Sakshaug and Slagstad, 1991; Goldman, 1993). In nutrient-limited areas, such as basins, primary producers shift from micro-sized autotrophic organisms (diatoms) to pico-sized mixotrophic plankton (flagellates) (Ardyna et al., 2011, 2017; Tremblay et al., 2009). Therefore, changes in the microplankton community composition associated with sea ice change affect primary production, carbon fixation, and higher trophic level organisms. Considering its importance, a comprehensive evaluation should be conducted in the Pacific Arctic Ocean. However, most studies on phytoplankton in the Pacific Arctic Ocean are based on short-term observations confined to specific locations or did not evaluate the effect of sea ice reduction. For example, early sea ice melt timing induces a decrease in ice algae abundance from the northern Bering Sea to Beaufort Sea (Fukai et al., 2021). In the northern Bering Sea, diatom composition changes from sea ice-associated species to cosmopolitan species due to early sea ice melt timing (Fukai et al., 2019). In a broader area (e.g., Chukchi Sea and Beaufort Sea) of the Pacific Arctic Ocean, phytoplankton species composition and biomass are examined from spring to autumn (Sukhanova et al., 2009; Sergeeva et al., 2010), but the effects of sea ice reduction have not been sufficiently evaluated. In addition, even in cases where the effects of sea ice have been evaluated, most studies have been based on pigment analysis and satellite data. For example, Coupel et al. (2012) and Fujiwara et al. (2014) evaluated the effect of sea ice reduction on phytoplankton in the Pacific Arctic Ocean, but both studies were based on pigment analysis and did not provide detailed information on changes in species composition. Thus, our understanding of the effect of sea ice reduction on microplankton community composition and distribution across the entire Pacific Arctic Ocean remains limited.

This study aimed to elucidate the effect of sea ice reduction on the microplankton community in the Pacific Arctic Ocean. To examine the effect of sea ice melt timing on the microplankton community in the Pacific Arctic Ocean using data from two different years (2019 vs. 2020), we hypothesize that sea ice melt timing affects autumn hydrography and microplankton community composition.

2. Materials and methods

2.1. Field samplings

Surveys were conducted in the Chukchi Sea and Canada Basin of the Pacific Arctic Ocean from October 8 to 28, 2019, and October 8 to 21, 2020, during the cruises of R/V *Mirai*, by the Japan Agency for Marine-Earth Science and Technology (Fig. 1, Supplementary Table 1). Water samples (1 L) were collected from the surface and the sub-surface chl. *a* maximum layer (SCM) (5.4–49.8 m) using buckets and Niskin bottles at 36 stations (including those sampled multiple times: St. 19_39 [seven times], St. 19_40 [two times], St. 19_41 [two times], and St. 19_42 [two times]) in 2019 and 20 stations in 2020. The samples (112 in total) were fixed with acid Lugol's (final concentration of 1 %). Simultaneously with

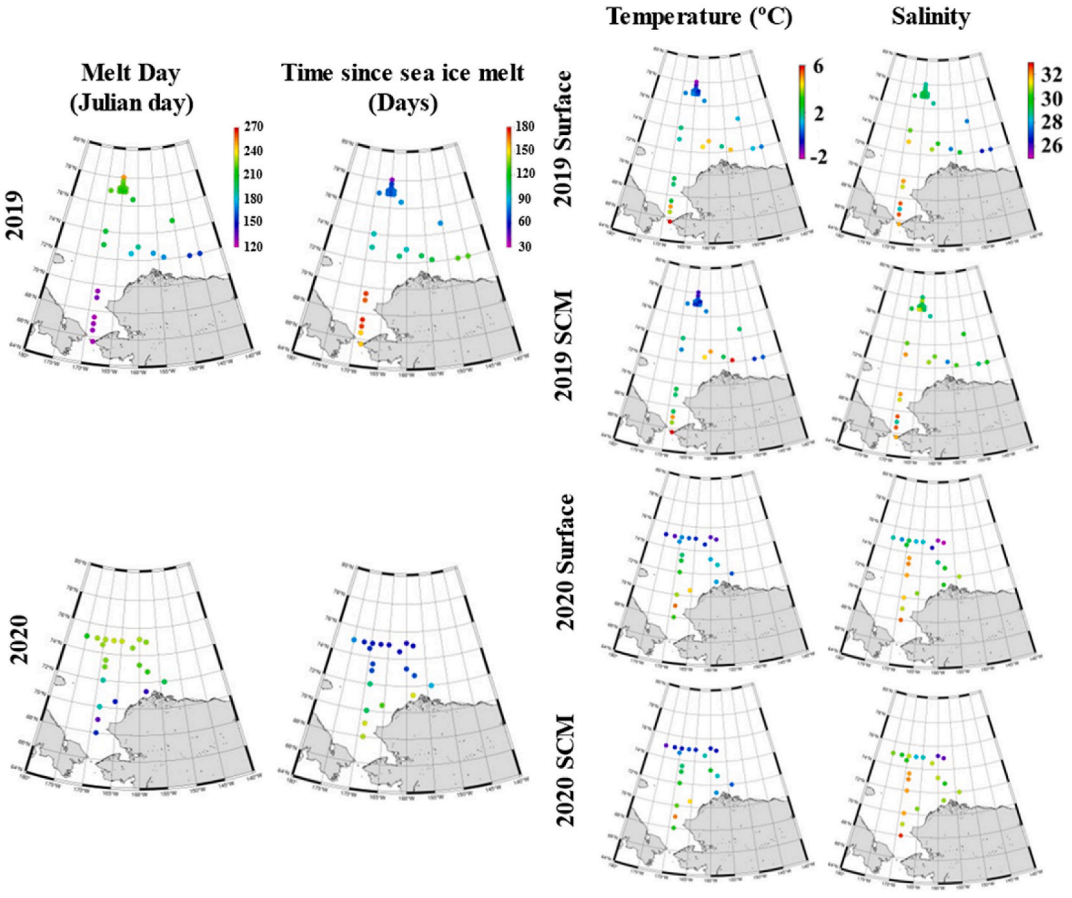

Fig. 2. Horizontal distribution of melting day, time since sea ice melting, temperature, and salinity at the surface and sub-surface chlorophyll maximum layer in the Pacific sector of the Arctic Ocean during autumn 2019 and 2020.

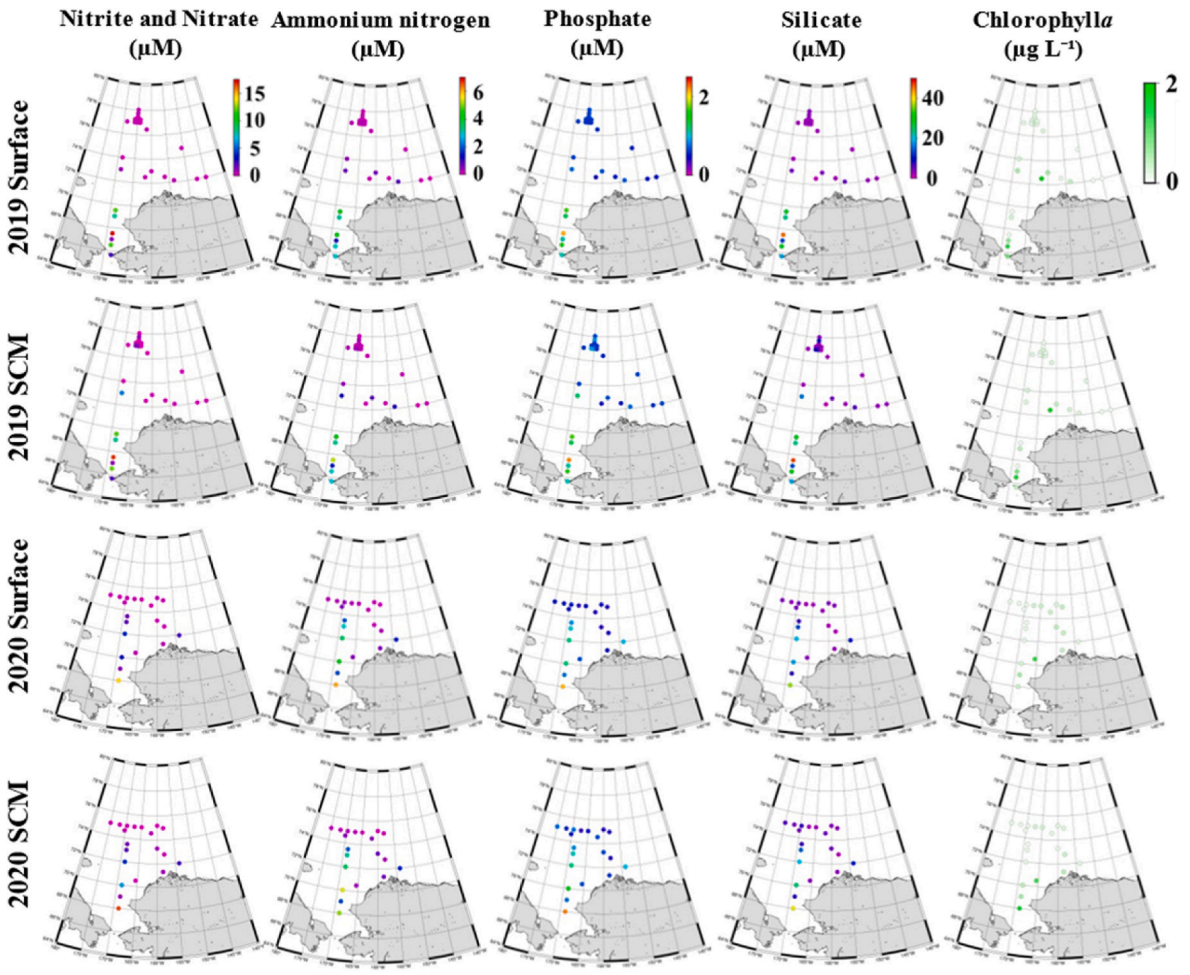

Fig. 3. Horizontal distribution of nutrients and chlorophyll *a* at the surface and sub-surface chlorophyll maximum layer in the Pacific sector of the Arctic Ocean during autumn 2019 and 2020.

water sampling, vertical profiles of water temperature, salinity, and chl. *a* fluorescence values were obtained using conductivity–temperature–depth (CTD) measurements (SBE-9plus, SBE-3plus, and SBE-4C). Water samples for nutrient concentrations were collected in duplicate Spitz tubes (10 mL) from the same depth as the water samples, and the concentrations of nitrate, nitrite, ammonium, phosphate, and silicate were measured using an autoanalyzer (QuAAtro 2HR, BLTEC Inc., Osaka, Japan) on board. In addition, the water samples for chl. *a* concentration were collected and filtered through a glass fiber filter (GF/F, pore size 0.7 μm, Whatman), immersed in *N-N* dimethylformamide (Wako Pure Chemical Industries, Ltd.), and maintained in the dark for at least 24 h to extract chl. *a*. After extraction, the chl. *a* concentration was measured in 2019 using the method by Holm-Hansen et al. (1965) and in 2020 using the method by Welschmeyer (1994) with a fluorometer (10-AU, Turner Designs Inc.).

2.2. Sample analysis

The fixed samples were concentrated 46–69 × using siphon tubes (Sukhanova, 1978). From the concentrated samples, 500 μL was mounted on a ruled glass slide using a micropipette, identified, and counted under an inverted microscope (ECLIPSE Ts2R, Nikon) at 200–400 × magnification. Diatoms, ciliates, and silicoflagellates were identified at the lowest possible levels (species or genus), and dinoflagellates were identified at the taxon level according to the methods proposed by Hasle and Syvertsen (1997), Hoppenrath et al. (2009), Maeda (1997), and Taniguchi (1997). The cells were counted using a minimum of 300 cells per sample.

2.3. Satellite data

The AMSER-2 sea ice concentration products provided by the JAXA Earth Observation Research Center were obtained using an online visualization application of the Arctic Data Archive System (https://ads.nipr.ac.jp/). Melt days were defined as the final days when sea ice concentration decreased below 15 %. Time since sea-ice melt (TSM) was defined as the period between the final day when the sea ice concentration decreased below 15 % and the sampling date.

2.4. Data analysis

The water masses in the study area were divided into three categories: Bering–Chukchi Summer Water (BCSW), characterized by temperatures ranging from 0 to 7 °C and salinity levels of 30–33.5; Bering–Chukchi Winter Water (BCWW) with temperatures ranging from −2 to 0 °C and salinity levels of 30–33.5; and Melt Water (MW) which exhibits temperatures from −2 to 7 °C and salinity levels of 25–30, as described by Danielson et al. (2017).

To reduce bias for abundant species, the cell density data (X: cells L^{-1}) for each taxon/species were transformed to $\sqrt[4]{X}$ prior to cluster analysis (Quinn and Keough, 2002). Similarities between samples were examined using the Bray–Curtis index based on differences in species composition. To group the samples, similarity indices were coupled using hierarchical agglomerative clustering with a complete linkage

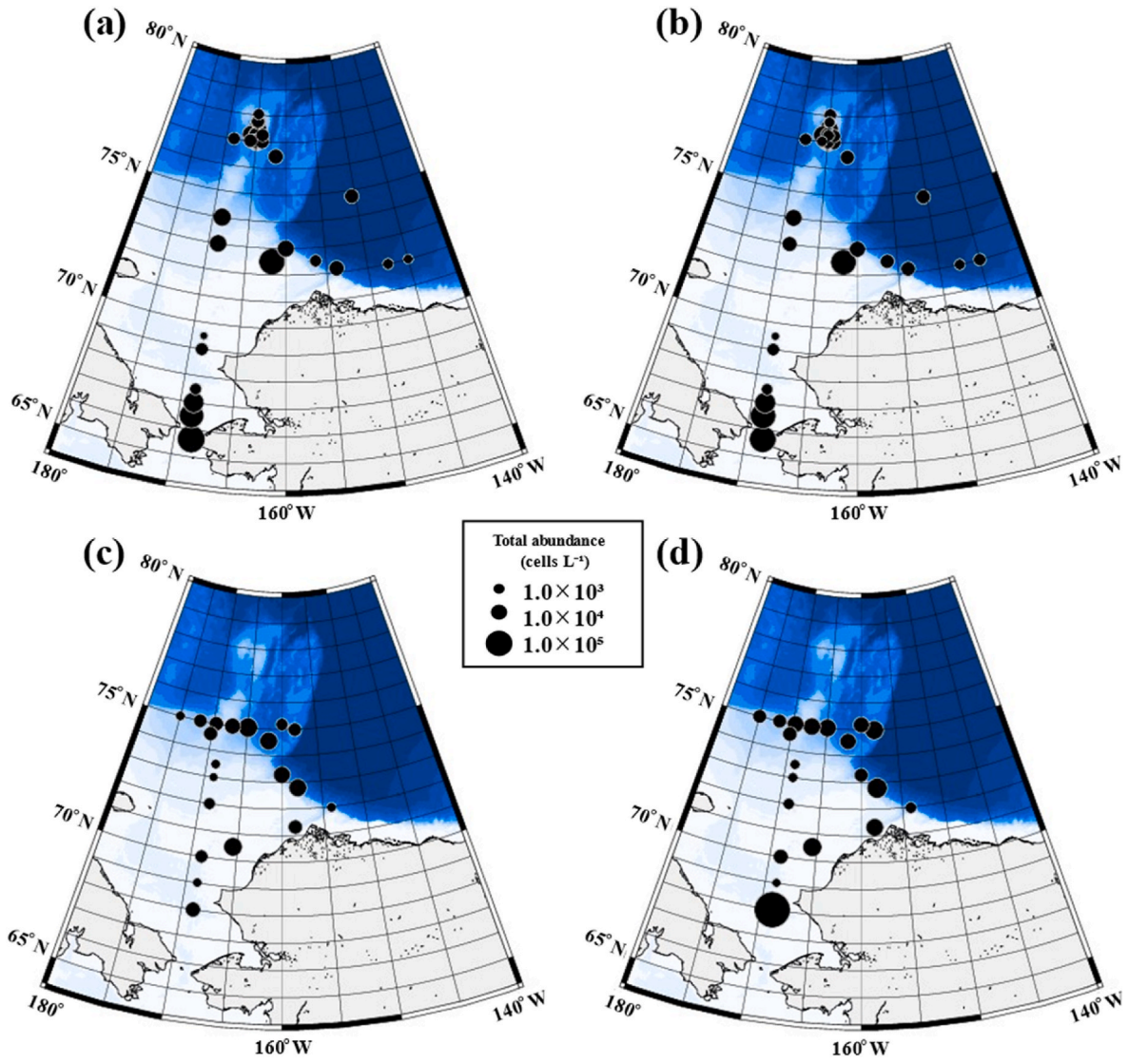

Fig. 4. Horizontal distribution of the total abundance of protists at the surface (a and c) and chlorophyll *a* maximum layer (b and d) in the Pacific sector of the Arctic Ocean during autumns 2019 (a and b) and 2020 (c and d).

method (an unweighted pair group method using the arithmetic mean) (Field et al., 1982). Similarity percentage (SIMPER) analysis was performed to determine the species that contributed to the top 50 % of total abundance for each group. Cluster and SIMPER analyses were conducted using PRIMER 7. A max-t test was conducted to evaluate the differences in sea ice melt dates and hydrographic parameters among the groups (Herberich et al., 2010). The tests were conducted using R software with the packages "multcomp" and "sandwich" (version 4.1.2, R Development Core Team, 2021).

The mixed layer depth at each station was defined as the depth at which the density changed by 0.03 σ from a depth of 5 m.

3. Results

3.1. Hydrography

The melt days were between May 6 and September 9, 2019, and between May 17 and August 21, 2020 (Fig. 2). A comparison of the melt days between the two stations located at approximately 73° N, 168.75° W revealed that St. 19_54 experienced a melt day on July 22, 2019, whereas St. 20_30 experienced a melt day on August 11, 2020. Based on this difference, we defined 2019 as the early sea ice melting year in the Pacific Arctic Ocean. The range of TSM was 40–175 days in 2019 and 55–145 days in 2020 (Fig. 2). The marginal ice zone was defined as north of 75° N in 2019 and at St. 20_11 and St. 20_12 in 2020 based on the sea ice distribution for each year.

Water temperature in 2019 and 2020 ranged from −1.6 to 6.4 °C and −1.1 to 5.3 °C, respectively, and were higher in the shelf area and lower in the basin in both years (Fig. 2). Salinity ranged from 26.5 to 32.5 and 25.2 to 32.7 in 2019 and 2020, respectively, and was higher in the shelf and lower in the marginal ice zone and Canada Basin in both years. In addition, localized low salinity was observed at St. 19_13 in the southern Chukchi Sea in 2019 (Fig. 2). For water mass distribution, in the shelf area of the southern Chukchi Sea, the BCSW was distributed on both the surface and SCM in both years. In the northern shelf area, the BCSW was observed in 2019, while the MW was observed in 2020 (Supplementary Fig. 1).

Regarding nutrients in 2019, nitrite and nitrate concentrations ranged from below the detection limit of −17.5 μM, ammonium from below the detection limit of −5.23 μM, phosphate from 0.45 to 2.24 μM, and silicate from 1.17 to 47.41 μM. In addition, these concentrations were relatively high at approximately 66–70° N, both at the surface and SCM (Fig. 3). In contrast, in 2020, nitrite and nitrate concentrations ranged from below the detection limit of −16.49 μM, ammonium from

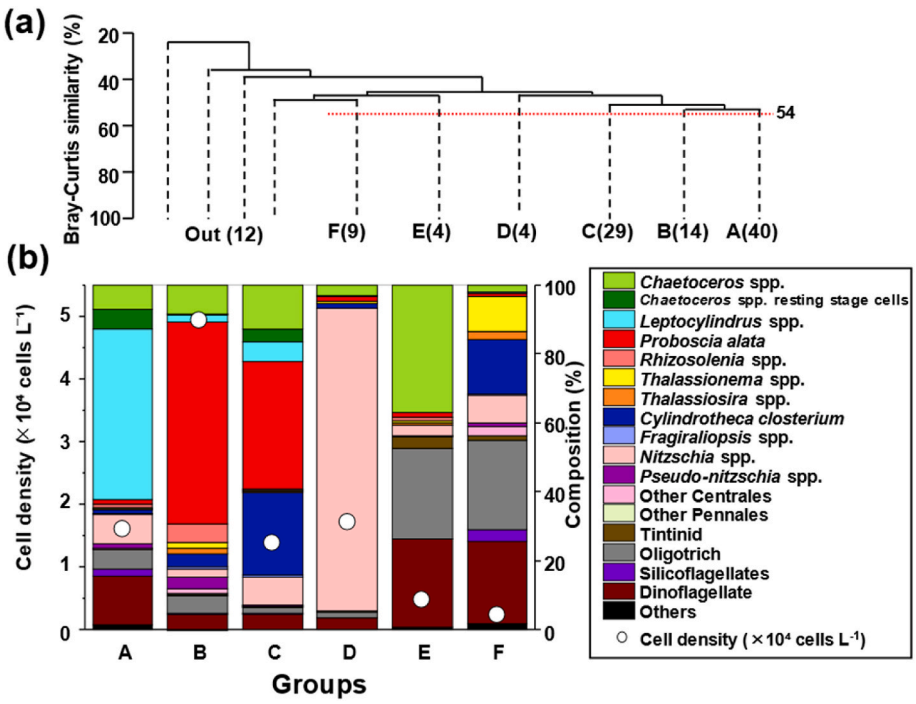

Fig. 5. Cluster analysis results based on protist abundance using Bray–Curtis similarity connected with unweighted pair group method using the arithmetic mean (a). Six groups (A–F) were identified with similarity at 54 % (dashed lines). Numbers in the parentheses indicate the number of stations included in each group. Mean abundance and species composition of each group (b).

below the detection limit of −6.05 μM, phosphate from below the detection limit of −2.24 μM, and silicate from 1.78 to 38.8 μM. These concentrations were relatively high at 68–72° N west of 165° W. The nutrient distribution showed similar trends in both years, with all nutrients observed to be low at the northern stations and the N:P ratio below 16 across the entire study area, indicating that all the stations were nitrogen-depleted (Fig. 3).

Chlorophyll *a* concentrations ranged from 0.1 to 1.9 μg L^{-1} and 0.1–1.7 μg L^{-1} in 2019 and 2020, respectively (Fig. 3). Localized high concentrations (1.9 μg L^{-1}) were observed in the surface layer of St. 19_25 (72.5° N, 161.7° W) in 2019. In 2020, the maximum value (1.7 μg L^{-1}) was observed in the SCM layer (58 m) of St. 20_35 (Fig. 3). Although certain stations had localized high chl. *a* concentrations, the overall trend was that chlorophyll concentrations were higher at stations in the south. The depth of the mixed layer ranged from 8 to 51 m for both years (Supplementary Table 1).

3.2. Cell density

Total microplankton cell densities were 110–1.6 × 10^5 cells L^{-1} in 2019 and 180–4.6 × 10^5 cells L^{-1} in 2020 (Fig. 4). The maximum value was detected in the surface layer at 0 m at St. 19_11 in 2019, and in the SCM layer at St. 20_35 in 2020. The comparison of total cell densities between the surface and SCM layers at the same stations throughout both years demonstrated similar patterns, with a correlation coefficient of 0.95 for total cell density between the surface and SCM at all stations except for St. 20_35. A total of 38 species belonging to 26 genera of diatoms (18 genera, 33 species in the central region, 7 genera, 4 species in the pennate) and 8 species belonging to 13 genera of ciliates were observed in both years (Supplementary Table 2). The cell density of diatoms was 144–4.6 × 10^5 cells L^{-1} at all stations, and the contribution in total cell density ranged from 13.3 to 100 %. Throughout both years, diatoms accounted for > 50 % of the total cell density at 95 stations, and diatoms dominated 85 % of all the stations. The cell density of dinoflagellates was 0–6.2 × 10^3 cells L^{-1} at all stations, and the total cell density ranged from 0 to 44 %.

3.3. Microplankton community

The cluster analysis showed that the microplankton community was categorized into six groups (A–F) according to a similarity of 54 % (Fig. 5a). Group A was distributed in the marginal ice zone (MIZ) in 2019, with an average total cell density of 1.7 × 10^4 cells L^{-1}, and primarily comprised *Leptocylindrus* spp., dinoflagellates, and oligotrich (Figs. 5b and 6). SIMPER analysis showed that contribution rates of these taxa were 14.4 %, 13.8 %, and 11.3 %, respectively (Table 1). Group B was distributed in the northern shelf area in 2019 and had a higher proportion of diatoms such as *Proboscia alata*, *Chaetoceros* spp., and *Pseudo-nitzschia* spp. (Fig. 5b and 6, Table 1). Total cell density was 5.0 × 10^4 cells L^{-1}, which was the highest among the six groups (Fig. 5b). Group C was distributed in the northern shelf area in 2020 and was dominated by diatoms such as *Cylindrotheca closterium*, *Chaetoceros* spp., and *Proboscia alata* (Fig. 5b and 6, Table 1). The total cell density was similar to that of group A (1.4 × 10^4 cells L^{-1}) (Fig. 5b). Group D was distributed at two stations in the margin ice zone in 2020, with a total cell density of 1.8 × 10^4 cells L^{-1}, and was dominated by the pennate diatom *Nitzschia* sp. 1 (Fig. 5b and 6, Table 1). Groups E and F were distributed in the Canada Basin at approximately 69° N (Fig. 6). Oligotrich and dinoflagellates were dominant, and the total cell density was low (Group E: 5.4 × 10^3 cells L^{-1}, Group F: 2.9 × 10^3 cells L^{-1}) (Fig. 5b).

The max-t test showed that all the environmental factors, except for nitrite and silicate, differed among the groups (Table 2). Group A, distributed in the MIZ, was characterized by a low water temperature (0.38 ± 0.70 °C), low salinity (29.26 ± 0.85), low chl. *a* (0.24 ± 0.06 μg L^{-1}), low nutrient concentration, and a relatively short TSM (75.85 ± 10.31 days) (Table 2). Group D, distributed in the MIZ, showed similar trends to group A but had significantly lower salinity (25.64 ± 0.39), ammonium concentration (0.07 ± 0.02 μM), and phosphate concentration (0.44 ± 0.20 μM), and a later melt day (228.00 ± 2.31 Julian day) and shorter TSM (57.00 ± 2.31 days) than group A (Table 2). Groups B and C exhibited apparent inter-annual differences in the northern shelf area, with significant differences observed in TSM, water

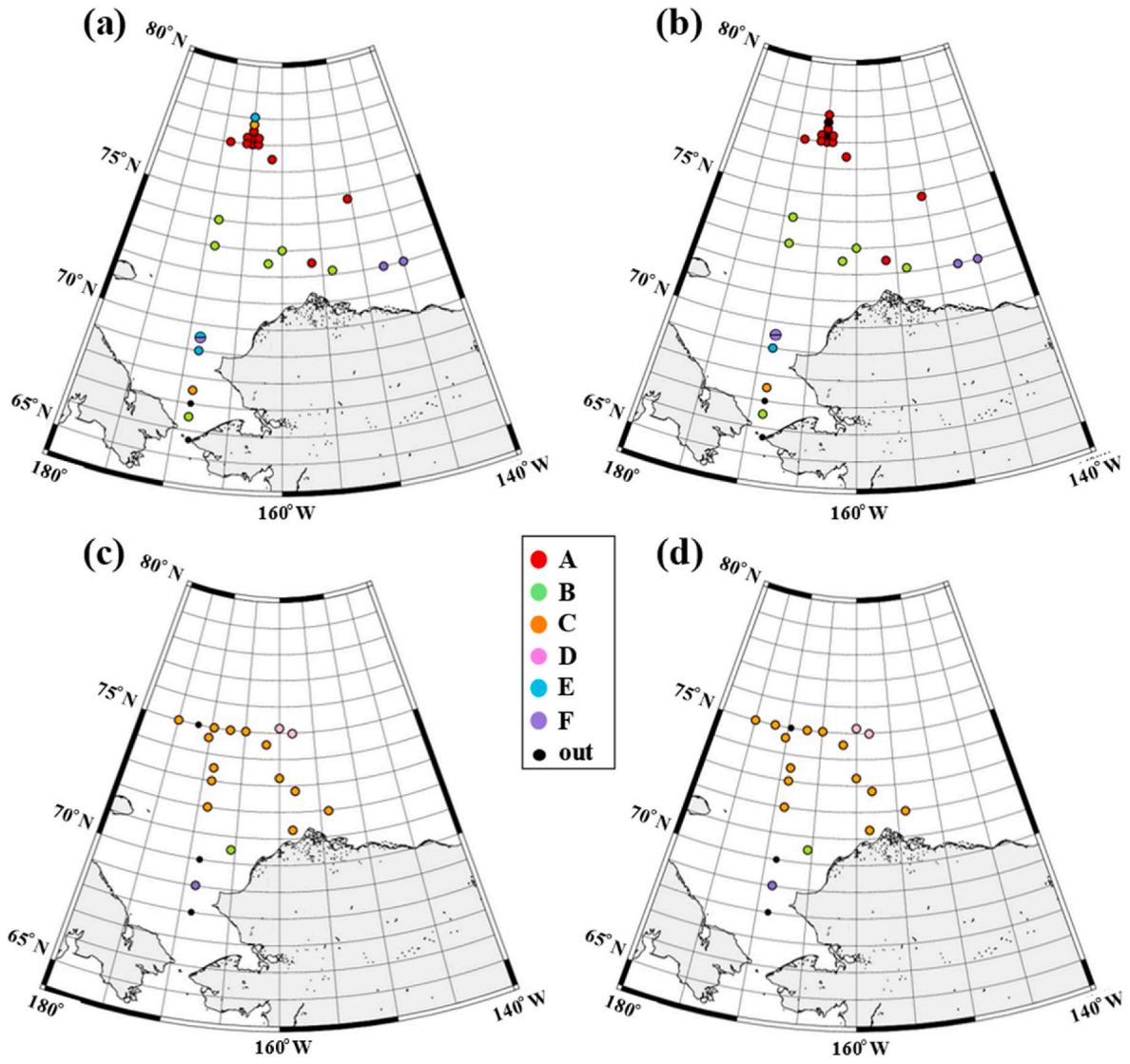

Fig. 6. Horizontal distributions of the six groups identified using Bray–Curtis similarity based on protist abundances (Fig. 5a) at the surface (a and c) and chlorophyll *a* maximum (b and d) in the Pacific sector of the Arctic Ocean during autumns 2019 (a and b) and 2020 (c and d).

temperature, and chl. *a*. Group B had an earlier sea ice melting date (176 vs. 208 Julian days), longer TSM (112 vs. 83 days), higher water temperature (3.75 vs. 0.99 °C), and higher chl. *a* (0.93 vs. 0.28) than group C (Table 2). Note that nitrite and nitrate concentrations in both groups were low (0.71 and 0.92 μM) excluding a St. 19_13 (11.54–11.93 μM) from group B and St. 19_71 (16.82–17.53 μM) from group C.

By comparing the vertical distribution of water temperature and salinity in each community, the stations in group B showed stratification owing to the warming of the surface layer. In contrast, the stations in 2020 showed stratification owing to the presence of surface water with low temperatures and salinity (Supplementary Figs. 2 and 3).

4. Discussion

4.1. Southern shelf

The southern Chukchi Sea shelf (south of 70° N) exhibited high total cell density and variability in community composition depending on the location in 2019 and at the SCM in 2020. The primary factors that influence the microplankton community in the southern Chukchi Sea include the advection of the Pacific warm water and river water (Walsh et al., 1989; Hill et al., 2005; Fukai et al., 2020). Nutrient-rich Anadyr Water (AW), characterized by cold temperatures and high salinity, comprises the BCSW and flows through the west side of the Bering Strait. In contrast, nutrient-depleted Alaskan Coastal Water (ACW), which is relatively warmer and fresher, flows through the eastern side of the Bering Strait from the Bering Sea (Coachman et al., 1975; Hansell et al., 1989; Danielson et al., 2017). The high salinity levels and relatively high nutrient concentrations at stations on the southern shelf indicate the distribution of AW. The high cell density in these stations was possibly sustained by the nutrient supply from AW (Walsh et al., 1989; Springer et al., 1996). In addition, low salinity water was present at St. 19_72 in 2019. Sea ice and river water are the two sources of freshwater in this area; however, the TSM of St. 19_72 was 172 days, which was more than 5 months after the sea ice retreated. Consequently, the low salinity was caused by the ACW, which carries a substantial amount of river water along the same longitudinal line as it meanders northward on the eastern side of the area (Springer and McRoy, 1993). In the adjacent northern Bering Sea, water masses and microplankton communities are closely related and change spatially synchronously, even in narrow areas (Fukai et al., 2020). Therefore, microplankton communities on the southern shelf of the Chukchi Sea vary among locations because different water masses flow from the south and change on a narrow spatial scale.

Table 1
SIMPER analysis results to confirm the dominant species in each group identified by cluster analysis (cf. Fig. 5) in the Pacific sector of the Arctic Ocean during autumn 2019 and 2020.

Groups	Species	Mean abundance (cells L^{-1})	Contrib. (%)
A	*Leptocylindrus* spp.	8205.2	14.35
	Dinoflagellate	2323.9	13.82
	Oligotrich	1001.0	11.31
	Nitzschia sp. 1	1445.7	9.49
	Chaetoceros spp.	1182.4	9.03
B	*Proboscia alata*	29263.2	12.57
	Chaetoceros spp.	4197.7	11.21
	Pseudo-nitzschia spp.	1699.6	10.31
	Cylindrotheca closterium	1840.8	9.83
	Dinoflagellate	2103.4	9.23
C	*Cylindrotheca closterium*	3485.5	19.19
	Chaetoceros spp.	1864.0	18.05
	Proboscia alata	5343.2	16.89
	Dinoflagellate	704.0	15.91
	Leptocylindrus spp.	797.5	11.43
D	*Nitzschia* sp. 1	15691.0	36.99
	Chaetoceros spp.	530.5	17.06
	Thalassionema spp.	177.1	13.12
	Cylindrotheca closterium	187.6	12.78
	Proboscia alata	214.7	7.61
E	Oligotrich	1413.9	24.77
	Dinoflagellate	1369.8	23.77
	Chaetoceros spp.	1976.6	18.85
	Rhizosolenia spp.	51.5	11.69
	Proboscia alata	82.1	7.49
F	Oligotrich	757.9	21.91
	Dinoflagellate	702.8	20.59
	Silicoflagellates	101.7	11
	Cylindrotheca closterium	467.7	9.5
	Thalassionema spp.	298.0	9.3

4.2. Northern shelf and slope

In the northern Chukchi Sea shelf and slope area, apparent interannual differences in the microplankton groups were observed: Group B dominated in 2019, and group C dominated in 2020. The difference in hydrography between the two groups was that group B experienced earlier sea ice melting (long TSM; 112.43 ± 21.58 days) and higher water temperature (3.75 ± 1.62 °C), whereas group C experienced later sea ice melting (short TSM; 82.79 ± 34.27 days) and distributed low-temperature (0.99 ± 1.22 °C) and relatively low salinity (30.21 ± 1.60) sea ice melted water.

Group B primarily comprised diatoms *Proboscia alata*, *Chaetoceros* spp., and *Pseudo-nitzschia* spp. In particular, St. 19_25 exhibited the highest cell density (1.3×10^5 cells L^{-1}) in group B, and the large diatom *P. alata* accounted for 80 % (1.0×10^5 cells L^{-1}) of the total cell density. In the Bering Sea shelf, a high cell density (7.0×10^5 cells L^{-1}) with a patchy distribution of *P. alata* was observed from late spring to summer (Sukhanova et al., 2006), and this study suggests that a similar phenomenon may occur in the northern Chukchi Sea. Sukhanova et al. (2006) concluded that the formation of localized high cell densities could be attributed to improved light availability and nutrient depletion associated with stratification owing to surface warming. *Proboscia alata* can assimilate silicate using ammonia and the organic nitrogen compound urea, even in environments with low nitrate concentrations (Goering and Iverson, 1981), which may promote the predominance of species with high organic nitrogen rather than inorganic nitrogen. The surface layer at St. 19_25 had a well-developed thermocline and a low nitrite and nitrate concentration of 0.19 μM. Other stations where group B was distributed also showed a low average nitrite and nitrate concentration of 0.71 μM, excluding St.19_13. Urea is the primary form of nitrogen excreted by zooplankton in the Arctic Ocean (Conover and Gustavson, 1999). Although urea was not measured in this study, a relatively high concentration of organic nitrogen (urea) can be estimated on the northern shelf and slope because of the high abundance of zooplankton in the Pacific Arctic Ocean (Abe et al., 2020). Comparing the nutrient demand within diatoms, small diatoms with large surface area/volume ratios were positively correlated with nitrate concentration, whereas large centric diatoms with small surface area/volume ratios, such as *P. alata*, were positively correlated with silicate concentration (Alves-De-Souza et al., 2008). Alternatively, *P. alata* dominance could be attributed to nitrogen depletion at all stations, while silicate remained relatively abundant. Therefore, the formation of group B can be described as follows: early sea ice melting → surface temperature increase by solar radiation → development of the thermocline → depletion of inorganic nitrogen on the surface → proliferation of species that can utilize organic nitrogen compounds (*P. alata*). The dominance of *P. alata* sustained by organic nitrogen is suggested by references and background information; however, this should be examined by fieldwork in the future.

In contrast, the dominant species in group C in 2020 were diatoms *Cylindrotheca closterium*, *Chaetoceros* spp., and *P. alata*, with an average total cell density of 1.4×10^4 cells L^{-1}, which was lower than that of group B. *Cylindrotheca closterium*, which was the dominant species in group C, is a cosmopolitan species that is also found in sea ice (Hop et al., 2020). Therefore, this may be a species associated with sea ice in this area. The microplankton composition in the sea ice core was not investigated in this study; however, the volume of melted sea ice water was higher in group C than in group B (Supplementary Fig. 3), which could be attributed to the 1-month later melt day in group C (208.10 ± 32.41 Julian day) compared to that in group B (175.57 ± 26.85 Julian

Table 2
Comparison of environmental factors between the groups identified by cluster analysis (cf. Fig. 5) in the Pacific sector of the Arctic Ocean during autumn 2019 and 2020. Different superscript numbers indicate significant differences between groups. The superscript alphabets were added only on significant variables by the max-t test, and the order is from high to low alphabetically. No superscript alphabet means the inter-group difference in the variables was not significant. Values represent the mean ± S.D. Numbers in parentheses are the number of sampling dates belonging to each group.

Parameters	Groups					
	A (40)	B (14)	C (29)	D (4)	E (4)	F (9)
Melt day (Julian day)	217.05 ± 12.08^{b}	175.57 ± 26.85^{c}	208.10 ± 32.41^{b}	228.00 ± 2.31^{a}	$161.00 \pm 60.70^{c,d}$	142.22 ± 13.08^{d}
TSM (day)	75.85 ± 10.31^{c}	112.43 ± 21.58^{b}	82.79 ± 34.27^{c}	57.00 ± 2.31^{d}	$133.00 \pm 62.40^{a,b}$	145.33 ± 17.85^{a}
Temperature (°C)	$0.38 \pm 0.70^{b,c}$	3.75 ± 1.62^{a}	$0.99 \pm 1.22^{b,c}$	-0.72 ± 0.33^{c}	$1.85 \pm 2.67^{a,b,c}$	$2.44 \pm 2.19^{a,b}$
Salinity	29.26 ± 0.85^{b}	30.91 ± 0.90^{a}	$30.21 \pm 1.60^{a,b}$	25.64 ± 0.39^{c}	$30.22 \pm 1.18^{a,b}$	$29.89 \pm 2.03^{a,b}$
NO_2+NO_3 (μM)	0.26 ± 0.54	2.29 ± 4.25*1	2.04 ± 4.35*2	0.15 ± 0.16	4.71 ± 4.07	3.54 ± 5.00
NH_4-N (μM)	0.15 ± 0.08^{b}	0.94 ± 0.91^{a}	1.23 ± 1.48^{a}	0.07 ± 0.02^{c}	2.14 ± 1.51^{a}	1.70 ± 1.78^{a}
PO_4-P (μM)	0.64 ± 0.11^{a}	0.82 ± 0.38^{a}	0.77 ± 0.46^{a}	0.44 ± 0.20^{b}	1.03 ± 0.37^{a}	0.91 ± 0.46^{a}
Si $(OH)_4$ (μM)	3.45 ± 2.28	8.31 ± 9.78	9.06 ± 11.50	3.84 ± 0.23	15.48 ± 10.41	11.51 ± 10.95
Fluorescence	0.24 ± 0.06^{b}	0.93 ± 0.60^{a}	0.28 ± 0.12^{b}	0.32 ± 0.10^{b}	0.31 ± 0.16^{b}	0.25 ± 0.23^{b}

*1. Average concentration excluding St.19_13 is 0.71 μM.
*2. Average concentration excluding St.19_71 is 0.92 μM.

day). Melt day affects the magnitude and onset of spring blooms in the seasonal sea ice area (Leu et al., 2011; Fujiwara et al., 2016). Sea ice contains phytoplankton, mainly pennate diatoms. When the sea ice melts, it initiates a phytoplankton bloom (Nimei et al., 2011). Therefore, the TSM of group C, which was 1 month shorter than that of group B, retained a significant amount of sea ice water in the surface layer, resulting in a high density of sea ice-associated species in the area.In the southern shelf area, if strong winds (>15 m s^{-1}) blow in autumn, vertical mixing is physically enhanced, and nutrients are upwelled to the surface from a layer deeper than that of the halocline, resulting in the growth of diatoms on the surface (Crawford et al., 2020; Yokoi et al., 2016). A relatively shallow and weak stratification layer is required for this wind-driven mixing enhancement to facilitate nutrient supply (Nishino et al., 2015; Yokoi et al., 2016). However, the surface salinity of group C was 29.5, which is apparently lower than that of the range 31–32.7 reported by Yokoi et al. (2016). Strong stratification owing to meltwater prevents nutrient supply from the lower layers, resulting in lower autumn primary production (Nishino et al., 2015). In this study, group C had an average thickness of melted water depth of 27.5 m and a stratification index of 222.86 J m^{-2} (Ladd and Stabeno, 2012), which was higher than that of group B (108.00 J m^{-2}). From this difference, the remaining melted sea ice water on the surface possibly prevented the upwelling of nutrients deeper than that of the halocline to the surface, even when vertical mixing by wind occurred. Additionally, the average nitrite and nitrate concentration was 0.92 μM, excluding St.19_71, which showed unusually high values in group C. The reason for the low cell density in group C may be attributed to the following sequence: delayed sea ice melting results in thick melted water, which hinders nutrient supply from the lower layers. Consequently, phytoplankton growth is constrained by both low water temperature and insufficient nutrients.

4.3. Marginal ice zone

In the MIZ, group A was observed in 2019 and mainly comprised centric diatoms, *Leptocylindrus* spp. (*L. danicus* and *L. minimus*), dinoflagellates, and oligotrich ciliates. This group was characterized by a low water temperature (0.38 ± 0.70 °C), low salinity (29.26 ± 0.85), low chl. *a* concentration (0.24 ± 0.06 μg L^{-1}), low nutrient concentration, and a short TSM (75.85 ± 10.31 days). The dominant species in group A, *L. danicus* and *L. minimus,* are cosmopolitan species that are widely distributed worldwide and appear in the North Atlantic Ocean, South China Sea, offshore California, and around Japan (Casas et al., 1999; Chen, 1993; Cupp, 1943; Ishizaka et al., 1987; Kraberg et al., 2010). In the same area, during August and September 2010, they appeared in relatively large numbers (174–858 cells L^{-1} on average for the entire area) (Matsuno et al., 2014). These species were also dominant in the northern Bering Sea during the summer of 2017 and 2018, with high water temperatures, low salinity, low nutrient concentrations, and low chl. *a* concentrations (Fukai et al., 2020). As mentioned above, these features were observed in group A, indicating that water temperature does not influence the distribution range of these species. *Leptocylindrus danicus* occurs during the declining phase of the spring bloom (Hoppenrath et al., 2009). Consequently, group A may not characterize the MIZ but could be the group associated with nutrient depletion following bloom decline. As a biological feature, *Leptocylindrus danicus* can utilize urea under nitrate-limited conditions, similar to *P. alata* (Gao et al., 2020; Yang et al., 2016). Thus, the ability of these species to utilize various nutrients may have enabled them to proliferate in environments with low levels of inorganic nitrogen and become dominant in the group. Almost no occurrence of *P. alata* in the MIZ could be attributed to the water temperature. The *P. alata* cell density was higher in warmer years (maximum water temperature 4.1 °C) than in colder years (water temperature 1.3–1.9 °C) where the sea ice remained present (Sukhanova et al., 2006). We observed that the difference in water temperature between groups A and C (0.38 vs. 0.99 °C) indicates that *P. alata* was dominant in group C. However, it could not be dominant in group A, including MIZ, despite the inorganic nitrogen-poor environment. This finding indicates that *P. alata* may not be able to proliferate actively in the MIZ at low water temperatures.

In contrast, in 2020, group D, dominated by *Nitzschia* spp., was observed in the MIZ. Inter-annual hydrography changes in groups A and D showed that 10 days after the melt day could affect the lowest temperature (−0.72 ± 0.33 °C) and salinity (25.64 ± 0.39); however, this finding is not conclusively explained owing to the limited data from only two stations in group D. A high cell density of *Nitzschia* sp. 1 was also observed at St. 19_MIZ, the northernmost station in 2019. Hop et al. (2020) indicated that *Nitzschia frigida* was observed from sea ice cores collected from the Arctic Ocean. Although *Nitzschia* sp. 1 observed in this study could not be identified at the species level by optical microscopy, its abundance in the MIZ suggests that this species may also be associated with sea ice (Hop et al., 2020).

5. Conclusion

Hydrographical differences among the areas characterized the microplankton community in the Pacific Arctic Ocean during autumn. In the southern Chukchi Sea, high cell densities were observed even during autumn owing to the inflow of nutrient-rich Pacific waters. In the northern Chukchi Sea and slope, apparent inter-annual differences were observed in the microplankton community, indicating that cell density and composition varied with sea ice melting timing via hydrographical changes. Early sea ice melting stimulates the growth of phytoplankton (*P. alata* and *Leptocylindrus* spp.), which can utilize organic nitrogen compounds. In the MIZ, cold-adapting species, including ice algae, were present in both years. Ten-day differences in sea ice melt days were observed between the years, which affected in-situ hydrography but not the microplankton community in the region. Our findings indicate that the response of microplankton to sea ice melting, in terms of production and diversity, varies by region. This type of case study should continue to develop prediction models based on diversity.

CRediT authorship contribution statement

Kohei Sumiya: Writing – original draft, Visualization, Investigation. **Dai Sumiyoshi:** Writing – review & editing, Visualization, Investigation, Formal analysis. **Kazutoshi Sato:** Investigation. **Akihiko Murata:** Investigation, Data curation. **Shigeto Nishino:** Investigation, Data curation. **Kohei Matsuno:** Writing – review & editing, Supervision, Project administration, Methodology, Funding acquisition, Conceptualization.

Declaration of competing interest

The authors declare that they have no known competing financial interests or personal relationships that could have appeared to influence the work reported in this paper.

Acknowledgments

We thank the captain, officers, crew, and researchers onboard the R/V *Mirai* for their outstanding efforts during field sampling. This work was funded by the Arctic Challenge for Sustainability (ArCS; Program Grant Number JPMXD1300000000) and Arctic Challenge for Sustainability II (ArCS II; program grant number JPMXD1420318865) projects. This work was also supported by the Japan Society for the Promotion of Science (JSPS) KAKENHI [grant number JP21H02263 (B) and JP25H01177 (A)].

Appendix A. Supplementary data

Supplementary data to this article can be found online at https://doi.

org/10.1016/j.polar.2025.101255.

References

Aagaard, K., Coachman, L.K., Carmack, E., 1981. On the halocline of the Arctic Ocean. Deep-Sea Res. A, Oceanogr. Res. Pap. 28, 529–545. https://doi.org/10.1016/0198-0149(81)90115-1.

Abe, Y., Matsuno, K., Fujiwara, A., Yamaguchi, A., 2020. Review of spatial and inter-annual changes in the zooplankton community structure in the western Arctic Ocean during summers of 2008–2017. Prog. Oceanogr. 186, 102391. https://doi.org/10.1016/j.pocean.2020.102391.

Alves-De-Souza, C., González, M.T., Iriarte, J.L., 2008. Functional groups in marine phytoplankton assemblages dominated by diatoms in fjords of southern Chile. J. Plankton Res. 30, 1233–1243. https://doi.org/10.1093/plankt/fbn079.

Ardyna, M., Gosselin, M., Michel, C., Poulin, M., Tremblay, J.É., 2011. Environmental forcing of phytoplankton community structure and function in the Canadian High Arctic: contrasting oligotrophic and eutrophic regions. Mar. Ecol. Prog. Ser. 442, 37–57. https://doi.org/10.3354/meps09378.

Ardyna, M., Babin, M., Gosselin, M., Devred, E., Rainville, L., Tremblay, J.É., 2014. Recent Arctic Ocean sea ice loss triggers novel fall phytoplankton blooms. Geophys. Res. Lett. 41, 6207–6212. https://doi.org/10.1002/2014GL061047.

Ardyna, M., Babin, M., Devred, E., Forest, A., Gosselin, M., Raimbault, P., Tremblay, J.É., 2017. Shelf-basin gradients shape ecological phytoplankton niches and community composition in the coastal Arctic Ocean (Beaufort Sea). Limnol. Oceanogr. 62, 2113–2132. https://doi.org/10.1002/lno.10554.

Arrigo, K.R., van Dijken, G.L., 2015. Continued increases in Arctic Ocean primary production. Prog. Oceanogr. 136, 60–70. https://doi.org/10.1016/j.pocean.2015.05.002.

Arrigo, K.R., van Dijken, G.L., Pabi, S., 2008. Impact of a shrinking Arctic ice cover on marine primary production. Geophys. Res. Lett. 35, 1–6. https://doi.org/10.1029/2008GL035028.

Arrigo, K.R., Perovich, D.K., Pickart, R.S., Brown, Z.W., van Dijken, G.L., Lowry, K.E., Mills, M.M., Palmer, M.A., Balch, W.M., Bates, N.R., Benitez-Nelson, C.R., Brownlee, E., Frey, K.E., Laney, S.R., Mathis, J., Matsuoka, A., Mitchell, B.G., Moore, G.W.K., Reynolds, R.A., Sosik, H.M., Swift, J.H., 2014. Phytoplankton blooms beneath the sea ice in the Chukchi sea. Deep Sea Res. II 105, 1–16. https://doi.org/10.1016/j.dsr2.2014.03.018.

Casas, B., Varela, M., Bode, A., 1999. Seasonal succession of phytoplankton species on the coast of A Coruña (Galicia, northwest Spain). Bol. Inst. Esp. Oceanogr. 15, 413–429.

Chen, W., 1993. Population ecology of *Leptocylindrus danicus* in Dapeng Bay, north of South China Sea. Mar. Sci. Bull. 12, 39–45.

Coachman, L.K., Aagaard, K., Tripp, R.B., 1975. Bering Strait: the Regional Physical Oceanography. University of Washington Press, Seattle, Washington.

Comiso, J.C., Parkinson, C.L., Gersten, R., Stock, L., 2008. Accelerated decline in the Arctic sea ice cover. Geophys. Res. Lett. 35, L01703. https://doi.org/10.1029/2007GL031972.

Conover, R.J., Gustavson, K.R., 1999. Sources of urea in arctic seas: zooplankton metabolism. Mar. Ecol. Prog. Ser. 179, 41–54. https://doi.org/10.3354/meps179041.

Coupel, P., Jin, H.Y., Joo, M., Horner, R., Bouvet, H.A., Sicre, M.A., Gascard, J.C., Chen, J.F., Garçon, V., Ruiz-Pino, D., 2012. Phytoplankton distribution in unusually low sea ice cover over the Pacific Arctic. Biogeosciences 9, 4835–4850. https://doi.org/10.5194/bg-9-4835-2012.

Crawford, A.D., Krumhardt, K.M., Lovenduski, N.S., van Dijken, G.L., Arrigo, K.R., 2020. Summer high-wind events and phytoplankton productivity in the Arctic Ocean. J. Geophys. Res. Oceans 125, e2020JC016565. https://doi.org/10.1029/2020JC016565.

Cupp, E.E., 1943. Marine Plankton Diatoms of the West Coast of North America. University of California Press, Berkeley, California.

Danielson, S.L., Eisner, L., Ladd, C., Mordy, C., Sousa, L., Weingartner, T.J., 2017. A comparison between late summer 2012 and 2013 water mass, macronutrients, and phytoplankton standing crops in the northern Bering and Chukchi. Deep Sea Res. II 135, 7–26. https://doi.org/10.1016/j.dsr2.2016.05.024.

Field, J.G., Clarke, K.R., Warwick, R.M., 1982. A practical strategy for analysing multispecies distribution patterns. Mar. Ecol. Prog. Ser. 8, 37–52. https://www.jstor.org/stable/24814621.

Fujiwara, A., Hirawake, T., Suzuki, K., Eisner, L., Imai, I., Nishino, S., Kikuchi, T., Saitoh, S.I., 2016. Influence of timing of sea ice retreat on phytoplankton size during marginal ice zone bloom period on the Chukchi and Bering shelves. Biogeosciences 13, 115–131. https://doi.org/10.5194/bg-13-115-2016.

Fujiwara, A., Hirawake, T., Suzuki, K., Imai, I., Saitoh, S.I., 2014. Timing of sea ice retreat can alter phytoplankton community structure in the western Arctic Ocean. Biogeosciences 11, 1705–1716. https://doi.org/10.5194/bg-11-1705-2014.

Fukai, Y., Abe, Y., Matsuno, K., Yamaguchi, A., 2020. Spatial changes in the summer diatom community of the northern Bering Sea in 2017 and 2018. Deep Sea Res. II 181–182, 104903. https://doi.org/10.1016/j.dsr2.2020.104903.

Fukai, Y., Matsuno, K., Fujiwara, A., Suzuki, K., Richlen, M.L., Fachon, E., Anderson, D. M., 2021. Impact of sea-ice dynamics on the spatial distribution of diatom resting stages in sediments of the Pacific Arctic Region. J. Geophys. Res. Oceans 126, e2021JC017223. https://doi.org/10.1029/2021JC017223.

Fukai, Y., Matsuno, K., Fujiwara, A., Yamaguchi, A., 2019. The community composition of diatom resting stages in sediments of the northern Bering Sea in 2017 and 2018: the relationship to the interannual changes in the extent of the sea ice. Polar Biol. 42, 1915–1922. https://doi.org/10.1007/s00300-019-02552-x.

Gao, P., Wang, P., Chen, S., Bi, W., Lu, S., He, J., Wang, X., Li, K., 2020. Effect of Ambient nitrogen on the growth of phytoplankton in the Bohai Sea: kinetics and parameters. J. Geophys. Res. Biogeosci. 125, 1–15. https://doi.org/10.1029/2020JG005643.

Giesbrecht, K.E., Varela, D.E., Wiktor, J., Grebmeier, J.M., Kelly, B., Long, J.E., 2019. A decade of summertime measurements of phytoplankton biomass, productivity and assemblage composition in the Pacific Arctic Region from 2006 to 2016. Deep Sea Res. II 162, 93–113. https://doi.org/10.1016/j.dsr2.2018.06.010.

Goering, J.J., Iverson, R.L., 1981. Phytoplankton distribution on the southeastern Bering Sea shelf. Eastern Bering Sea Shelf: Oceanograph. Res. 2, 933–946.

Goldman, J.C., 1993. Potential role of large oceanic diatoms in new primary production. Deep Sea Res. I 40, 159–168. https://doi.org/10.1016/0967-0637(93)90059-C.

Grebmeier, J.M., McRoy, C.P., Feder, H.M., 1988. Pelagic-benthic coupling on the shelf of the northern Bering and Chukchi Seas. I. Food supply source and benthic biomass. Mar. Ecol. Prog. Ser. 48, 57–67. https://www.jstor.org/stable/24827622.

Grebmeier, J.M., Cooper, L.W., Feder, H.M., Sirenko, B.I., 2006. Ecosystem dynamics of the pacific-influenced Northern bering and Chukchi Seas in the Amerasian Arctic. Prog. Oceanogr. 71, 331–361. https://doi.org/10.1016/j.pocean.2006.10.001.

Hansell, D.A., Goering, J.J., Walsh, J.J., McRoy, C.P., Coachman, L.K., Whitledge, T.E., 1989. Summer phytoplankton production and transport along the shelf break in the Bering Sea. Cont. Shelf Res. 9, 1085–1104. https://doi.org/10.1016/0278-4343(89)90060-5.

Hasle, G.R., Syvertsen, E.E., 1997. Marine diatoms. In: Tomas, C.R. (Ed.), Identifying Marine Phytoplankton. Academic Press, San Diego, pp. 5–385.

Herberich, E., Sikorski, J., Hothorn, T., 2010. A robust procedure for comparing multiple means under heteroscedasticity in unbalanced designs. PLoS One 5, e9788. https://doi.org/10.1371/journal.pone.0009788.

Hill, V., Cota, G., 2002. Spatial patterns of primary production on the shelf, slope and basin of the Western Arctic in 2002. Deep Sea Res. II 52, 24–26. https://doi.org/10.1016/j.dsr2.2005.10.001.

Hill, V., Cota, G., Stockwell, D., 2005. Spring and summer phytoplankton communities in the Chukchi and Eastern Beaufort Seas. Deep Sea Res. II 52, 3369–3385. https://doi.org/10.1016/j.dsr2.2005.10.010.

Holm-Hansen, O., Lorenzen, C.J., Holmes, R.W., Strickland, J.D., 1965. Fluorometric determination of chlorophyll. ICES. J. Mar. Sci. 30, 3–15. https://doi.org/10.1093/icesjms/30.1.3.

Hop, H., Vihtakari, M., Bluhm, B.A., Assmy, P., Poulin, M., Gradinger, R., Peeken, I., von Quillfeldt, C., Olsen, L.M., Zhitina, L., Melnikov, I.A., 2020. Changes in sea-ice protist diversity with declining sea ice in the Arctic Ocean from the 1980s to 2010s. Front. Mar. Sci. 7, 243. https://doi.org/10.3389/fmars.2020.00243.

Hoppenrath, M., Elbrächter, M., Drebes, G., 2009. Marine Phytoplankton: Selected Microphytoplankton Species from the North Sea Around Helgoland and Sylt. Schweizerbart Science Publishers, Frankfurt, Germany.

Horner, R., Schrader, G.C., 1982. Relative contributions of ice algae, phytoplankton, and benthic microalgae to primary production in nearshore regions of the Beaufort Sea. Arctic 35, 485–503. https://www.jstor.org/stable/40509382.

Horner, R., 1984. Phytoplankton abundance, chlorophyll *a*, and primary production in the western Beaufort sea. In: Barnes, P.W., Schell, D.M., Reimnitz, E. (Eds.), The Alaskan Beaufort Sea: Ecosystems and Environment. Academic Press, Orlando, Florida, pp. 295–310.

Ishizaka, J., Kaichi, M., Takahashi, M., 1987. Resting spore formation of *Leptocylindrus danicus* (Bacillariophyceae) during short time-scale upwelling and its significance as predicted by a simple model. Ecol. Res. 2, 229–242. https://doi.org/10.1007/BF02349776.

Kraberg, A., Baumann, M., Durselen, C.D., 2010. Coastal Phytoplankton: Photo Guide for Northern European Seas. Verlag Dr. Friedrich Pfeil, Munchen, Germany.

Kwok, R., Rothrock, D.A., 2009. Decline in Arctic sea ice thickness from submarine and ICESat records: 1958–2008. Geophys. Res. Lett. 36, L15501. https://doi.org/10.1029/2009GL039035.

Ladd, C., Stabeno, P.J., 2012. Stratification on the Eastern Bering Sea shelf revisited. Deep Sea Res. II 65–70, 72–83. https://doi.org/10.1016/j.dsr2.2012.02.009.

Leu, E., Soreide, J.E., Hessen, D.O., Falk-Petersen, S., Berge, J., 2011. Consequences of changing sea–ice cover for primary and secondary producers in the European Arctic shelf seas: timing, quantity, and quality. Prog. Oceanogr. 90, 18–32. https://doi.org/10.1016/j.pocean.2011.02.004.

Lewis, K.M., van Dijken, G.L., Arrigo, K.R., 2020. Changes in phytoplankton concentration now drive increased Arctic Ocean primary production. Science 369, 198–202. https://doi-org.ezoris-hokudai.idm.oclc.org/10.1126/science.aay8380.

Maeda, M., 1997. Suborder Oligotrichida. In: Chihara, M., Murano, M. (Eds.), An Illustrated Guide to Marine Plankton in Japan. Tokai University Press, Tokyo, pp. 397–420.

Matsuno, K., Ichinomiya, M., Yamaguchi, A., Imai, I., Kikuchi, T., 2014. Horizontal distribution of microprotist community structure in the western Arctic Ocean during late summer and early fall of 2010. Polar Biol. 37, 1185–1195. https://doi.org/10.1007/s00300-014-1512-z.

Matsuno, K., Yamaguchi, A., Nishino, S., Inoue, J., Kikuchi, T., 2015. Short-term changes in the mesozooplankton community and copepod gut pigment in the Chukchi Sea in autumn: reflections of a strong wind event. Biogeosciences 12, 4005–4015. https://doi.org/10.5194/bg-12-4005-2015.

McLaughlin, F.A., Carmack, E.C., 2010. Deepening of the nutricline and chlorophyll maximum in the Canada Basin interior, 2003–2009. Geophys. Res. Lett. 37, L24602. https://doi.org/10.1029/2010GL045459.

McRoy, C.P., 1993. ISHTAR, the project: an overview of inner Shelf transfer and recycling in the bering and Chukchi seas. Cont. Shelf Res. 13, 473–479. https://doi.org/10.1016/0278-4343(93)90091-B.

Nimei, A., Michel, C., Hille, K., Poulin, M., 2011. Protist assemblages in winter sea ice: setting the stage for the spring ice algal bloom. Polar Biol. 34, 1803–1817. https://doi.org/10.1007/s00300-011-1059-1.

Nishino, S., Kawaguchi, Y., Inoue, J., Hirawake, T., Fujiwara, A., Futsuki, R., Onodera, J., Aoyama, M., 2015. Nutrient supply and biological response to wind-induced mixing, inertial motion, internal waves, and currents in the northern Chukchi sea. J. Geophys. Res. Oceans 120, 1975–1992. https://doi.org/10.1002/2014JC010407.

Pabi, S., van Dijken, G.L., Arrigo, K.R., 2008. Primary production in the Arctic Ocean, 1998–2006. J. Geophys. Res. Oceans 113, C08005. https://doi.org/10.1029/2007JC004578.

Quinn, G.P., Keough, M.J., 2002. Experimental Design and Data Analysis for Biologists. Cambridge University Press, New York.

Sakshaug, E., 1997. Biomass and productivity distributions and their variability in the Barents Sea. ICES J. Mar. Sci. 54, 341–350. https://doi.org/10.1006/jmsc.1996.0170.

Sakshaug, E., Slagstad, D., 1991. Light and productivity of phytoplankton in polar marine ecosystems: a physiological view. Polar Res. 10, 69–86. https://doi.org/10.3402/polar.v10i1.6729.

Sergeeva, V.M., Sukhanova, I.N., Flint, M.V., Pautova, L.A., Grebmeier, J.M., Cooper, L. W., 2010. Phytoplankton community in the western Arctic in July–August 2003. Oceanology 50, 184–197. https://doi.org/10.1134/S0001437010020049.

Shiozaki, T., Fujiwara, A., Sugie, K., Nishino, S., Makabe, A., Harada, N., 2022. Bottom-associated phytoplankton bloom and its expansion in the Arctic Ocean. Glob. Change Biol. 28, 7286–7295. https://doi.org/10.1111/gcb.16421.

Springer, A.M., McRoy, C.P., 1993. The paradox of pelagic food webs in the northern Bering Sea III. Patterns of primary production. Cont. Shelf Res. 13, 575–599. https://doi.org/10.1016/0278-4343(93)90095-F.

Springer, A.M., McRoy, C.P., Flint, M.V., 1996. The Bering Sea Green Belt: shelf-edge processes and ecosystem production. Fish. Oceanogr. 5, 205–223. https://doi.org/10.1111/j.1365-2419.1996.tb00118.x.

Stroeve, J., Holland, M.M., Meier, W., Scambos, T., Serreze, M., 2007. Arctic sea ice decline: faster than forecast. Geophys. Res. Lett. 34, L09501. https://doi.org/10.1029/2007GL029703.

Sukhanova, I.N., 1978. 5.2.2 Settling without the inverted microscope. In: Sournia, A. (Ed.), Phytoplankton Manual. United Nations Educational, Scientific and Cultural Organization, Paris, p. 97.

Sukhanova, I.N., Flint, M.V., Pautova, L.A., Stockwell, D.A., Grebmeier, J.M., Sergeeva, V.M., 2009. Phytoplankton of the western Arctic in the spring and summer of 2002: structure and seasonal changes. Deep Sea Res. II 56, 1223–1236. https://doi.org/10.1016/j.dsr2.2008.12.030.

Sukhanova, I.N., Flint, M.V., Whitledge, T.E., Stockwell, D.A., Rho, T.K., 2006. Mass development of the planktonic diatom *Proboscia alata* over the Bering Sea shelf in the summer season. Oceanology 46, 200–216. https://doi.org/10.1134/S000143700602007X.

Taniguchi, A., 1997. Suborder tintinnina. In: Chihara, M., Murano, M. (Eds.), An Illustrated Guide to Marine Plankton in Japan. Tokai University Press, Tokyo, pp. 421–483.

Tremblay, G., Belzile, C., Gosselin, M., Poulin, M., Roy, S., Tremblay, J.É., 2009. Late summer phytoplankton distribution along a 3500 km transect in Canadian Arctic waters: strong numerical dominance by picoeukaryotes. Aquat. Microb. Ecol. 54, 55–70. https://doi.org/10.3354/ame01257.

Walsh, J.J., McRoy, C.P., Coachman, L.K., Goering, J.J., Nihoul, J.J., Whitledge, T.E., Blackburn, T.H., Parker, P.L., Wirick, C.D., Shuert, P.G., Grebmeier, J.M., Springer, A.M., Tripp, R.D., Hansell, D.A., Djenidi, S., Deleersnijder, E., Henriksen, K., Lund, B.A., Andersen, P., Müller-Karger, F.E., Dean, K., 1989. Carbon and nitrogen cycling within the Bering/Chukchi Seas: source regions for organic matter effecting AOU demands of the Arctic Ocean. Prog. Oceanogr. 22, 277–359. https://doi.org/10.1016/0079-6611(89)90006-2.

Welschmeyer, N.A., 1994. Fluorometric analysis of chlorophyll *a* in the presence of chlorophyll *b* and pheopigments. Limnol. Oceanogr. 39, 1985–1992. https://doi.org/10.4319/lo.1994.39.8.1985.

Yang, H.S., Jeon, S.G., Oh, S.J., 2016. Survival strategy of dominant diatom *Chaetoceros debilis* and *Leptocylindrus danicus* as southwestern parts of East sea-The availability of dissolved organic nitrogen under dissolved inorganic nitrogen-limited environments. J. Korean Soc. Mar. Environ. Saf. 22, 212–219. https://doi.org/10.7837/kosomes.2016.22.2.212.

Yokoi, N., Matsuno, K., Ichinomiya, M., Yamaguchi, A., Nishino, S., Onodera, J., Inoue, J., Kikuchi, T., 2016. Short-term changes in a microplankton community in the Chukchi Sea during autumn: consequences of a strong wind event. Biogeosciences 13, 913–923. https://doi.org/10.5194/bg-13-913-2016.

Zheng, L., Cheng, X., Chen, Z., Liang, Q., 2021. Delay in Arctic Sea Ice Freeze-Up linked to early summer Sea Ice loss: evidence from satellite observations. Remote Sens. 13, 2162. https://doi.org/10.3390/rs13112162.